

Compact Fiber Laser and Fiber Readout System for Multilayered Optical Memory

Masatoshi Tsuji¹, Wataru Inami^{2,4}, Yoshimasa Kawata^{3,4}

¹Research Fellow of the Japan Society for the Promotion of Science, Chiyoda, Tokyo 102-8472, Japan

²Division of Global Research Leaders, Shizuoka University, Hamamatsu 432-8561, Japan

³Faculty of Engineering, Shizuoka University, Hamamatsu 432-8561, Japan

⁴JST-CREST, Kawaguchi, Saitama 332-0012, Japan

¹tsuji@optsci.eng.shizuoka.ac.jp

²inami@eng.shizuoka.ac.jp

³kawata@eng.shizuoka.ac.jp

Abstract— We developed a compact and high-power mode-locked fiber laser for multilayered optical memories. The average power and pulse width of the output pulse from the fiber laser that we developed were 109 mW and 2.1 ps, respectively. The dispersion of the output pulse was compensated with an external single-mode fiber of 2.5 m length. The pulse was compressed from 2.1 ps to 93 fs by dispersion compensation. We proposed a fiber confocal microscope as an alignment-free readout system of multilayered optical memories. The fiber confocal microscope does not require fine pinhole position alignment because the fiber core is used as the point light source and the pinhole, and both of which are always located at the conjugated point. The configuration reduces the required accuracy of pinhole position alignment. The fiber confocal microscope can also achieve a compact pickup head. Recording layers in a multilayered medium could be detected with an axial resolution of approximately 900 nm. We demonstrated eight-layer readout with the fiber confocal microscope.

Keywords— Fiber laser, Fiber confocal microscope, Multilayered optical memory, Compact, Alignment-free system

I. INTRODUCTION

Optical memories are promising as data archival storage in many applications such as cloud computing and three-dimensional (3D) television. Optical memories have long time stability and lower power consumption. Recently, a blu-ray disc-type optical memory that had a capacity of over 100 Gbyte has been standardized. To realize further large data capacity, many technologies have been reported as next-generation optical memory, such as holographic memories[1,2], near-field recording technology using a solid-immersion lens (SIL)[3], super-resolution near-field structure (Super-RENS) technology[4], and multilayered optical memories[5-9].

Multilayered optical memories are one of the

most promising technologies for next-generation optical data storage. Multilayered optical memories can increase the recording capacity by increasing the number of recording layers. The technologies of current optical memories, such as optical pickups, servo and tracking systems, and aberration corrections, can be used for multilayered optical memories with some modifications and extensions. Recently, the development of a blu-ray disc with sixteen layers has been reported by Pioneer and TDK and the disc had 512 Gbyte recording capacity [10]. Surface plasmon techniques were also applied to multilayered optical memories to increase the recording capacity [11]. Zijlstra et al. reported a five-dimensional optical memory using 3D volume, wavelength, and polarization multiplex recording techniques[12].

We have developed a multilayered optical memory using a multilayered medium. Multilayered optical memories can increase the recording capacity by increasing the number of recording layers.

One of the key issues to realize multilayered optical memory is to realize a compact optical drive system. Conventional systems were consisted of a large size femtosecond laser and many optical components. In order to overcome this issue, we propose a recording and readout system using optical fibers. Because a fiber is possible to be bended, it has high flexibility in system configuration and becomes compact. We developed a fiber laser as a recording laser and a fiber

confocal microscope as readout system for multilayered optical memory.

II. DEVELOPMENT OF FIBER LASER

We developed a pulsed fiber laser for multilayer recording. Figure 1 shows optical setup of the fiber laser. Erbium doped fiber (EDF) was pumped by two 980 nm laser diodes (LDs) through wavelength division multiplexing (WDM) coupler. The power of each LD was 450 mW. The cavity comprised of EDF and single-mode fiber (SMF). Each fiber was spliced and the splicing loss was negligible. The monitor coupler picked up pulses for measuring the spectrum and pulse train. A polarization beam splitter (PBS) operated as the output port. The spectrum, average power, and temporal waveform of output pulses were measured by a spectrum analyzer, a power meter, and a two-photon absorption-type autocorrelator, respectively. Optical isolators were inserted to prevent the back-reflection in the cavity and to ensure the unidirectional operation. A SMF of 2.5 m length was used for dispersion compensation.

Figure 2(a) shows the spectrum of the output pulse from the PBS. The spectrum bandwidth was broadened by amplification at EDF. Figure 2(b) shows the spectrum of the output pulse from the monitor coupler. We can observe the well-defined spectrum with Gaussian distribution, as shown in Fig. 2(b). The center wavelength of the spectrum was about 1540 nm.

Figure 3 shows the pulse train measured at the monitor coupler. The time interval of pulse trains was 17.4 ns, and the repetition rate was 57.5 MHz. Figure 4 shows the temporal waveform of the output pulse from the PBS. The pulse shape was well defined and the pulse width was 2.1 ps. In order to increase the probability of the two photon absorption (TPA) process, the pulse width should be decreased.

In order to decrease the pulse width, we performed dispersion compensation to use a 2.5 m SMF. Figure 5 shows the temporal waveform of output pulse after dispersion compensation. By chirped pulse compensation, it was compressed the pulse width to 93 fs. We succeeded in operating with an average power of 90 mW and high-power

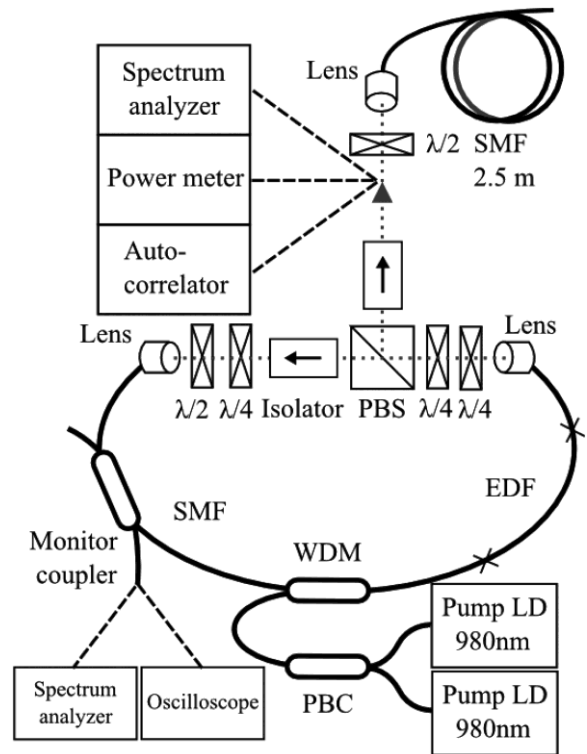
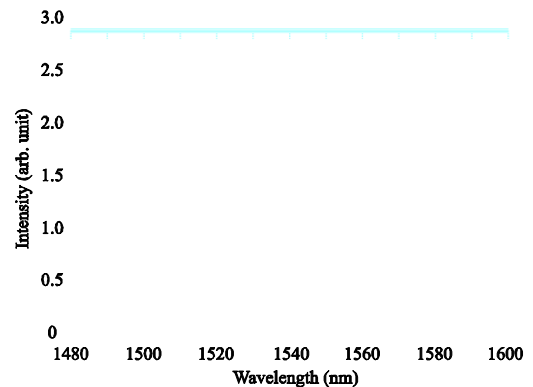


Fig. 1 Optical setup of fiber laser that we developed



(b)

Fig. 2 Spectrum of output pulse from monitor coupler: (a) spectrum of output pulse from PBS and (b) spectrum of output pulse from monitor coupler

Fig. 3 Pulse train from monitor coupler

Fig. 4 Temporal waveform of output pulse from PBS

pulse generation. The pulse energy was calculated as 1.6 nJ from the average power and repetition rate. We estimated that the peak power was 5.3 kW from the pulse shape and pulse energy.

III. THREE DIMENSIONAL RECORDING WITH FIBER LASER

We demonstrated TPA recording with the developed fiber laser in a photochromic recording material. The medium was fabricated with the casting method and this medium was a bulk-type. First, diarylethene (*cis*-1,2-dicyano-1,2-bis(2,4,5-trimethyl-3-thienyl)ethene) (DE) was heated over melting point. Then the melted DE was put between the two glass substrates. The thickness of recording layer was several μm and uniform medium could be fabricated. The entire medium is photosensitive, so recording bits will be created in any part of the medium. This allows no layers fabrication needed for the medium. DE is used because it has large TPA cross-sections in the near-infrared region.

Figure 6 shows the 3D recording demonstration

Fig. 5 Temporal waveform of output pulse after pulse compression

of DE sample. Two layers were recorded and observed. Figure 6(a) shows the 1st layer and (b) is the 2nd layer. Letter “A” and “B” was recorded in bit sequence for each layer respectively. The spacing between the layers was 40 μm . The recording power used was 4.7 mW with an exposure time of 8 ms focused into the media. The cross talk in the 2nd layer was observed due to the detection system do not incorporate confocal system. The confocal readout system can improve the contrast of readout data.

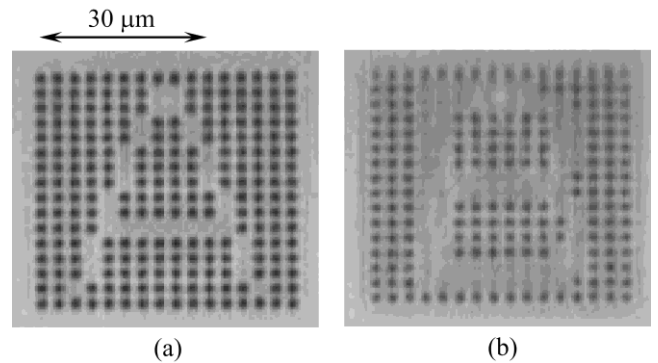


Fig. 6 3D recording with fiber laser that we developed

IV. FIBER CONFOCAL MICROSCOPE AS READOUT SYSTEM OF MULTILAYERED OPTICAL MEMORY

We propose a fiber confocal microscope for the alignment-free readout system of multilayered optical memories. In this fiber confocal microscope, a small fiber core serves as both the point light source and the pinhole to cut the scattered light from the defocused region. Because the point light source and the pinhole are always located at the same position, the fiber confocal system does not require the fine alignment of pinhole position. The

light scattered at the focal position of an objective lens is automatically focused at the fiber core. This reduces the required alignment accuracy.

The fiber confocal microscope can also achieve a compact pickup head. Since this system can comprise a fiber, the readout laser and the detector are located outside of the optical pickup or the optical drive. This reduces the number of optical components on pickup heads and small pickups in current optical memory systems. The fiber confocal microscope can also be combined with an ultrashort-pulse fiber laser as a recording light source of multilayered optical memories. The fiber confocal microscope is promising for the alignment-free and compact readout system of multilayered optical memories.

V. OPTICAL SETUP OF FIBER CONFOCAL MICROSCOPE

Figure 7 shows the optical setup of the fiber confocal microscope that we have developed. A helium-neon (He-Ne) laser of 633 nm wavelength was used for readout. The light was focused onto the SMF end and passed through the fiber coupler. The light emitted by the fiber was collimated using an objective of 0.65 numerical aperture (NA) and focused onto the multilayered medium using an oil-immersion objective of 1.3 NA. The signal reflected from the focal spot was focused at the fiber end with the same optics. The signal was separated using the fiber coupler and detected with a photomultiplier tube (PMT). The branch ratio of the fiber coupler was 50:50. The SMF model we used was SM600, Fibertec Ltd. The mode field diameter of the SMF was about 4.5 μm , which corresponded to the pinhole diameter. The multilayered medium was placed on an XYZ-axes translation stage controlled by a computer.

We introduced two noise reduction methods into the fiber confocal microscope. First, to reduce the reflection at the fiber end, we used an angled physical contact (APC) connector at the fiber end. The end face of the APC connector was cut with an angle slanted toward the optical axis. The reflected light at the fiber end did not propagate back in the fiber core. We reduced the reflected light at the end to less than 60 dB. Second, the signal and the

reflection light were separated by controlling the polarization state. We inserted a quarter-wave plates (QWPs) and a PBS into the light path. The linear polarization state of the signal was rotated 90° because it passed through the QWP twice. The reflected light at the fiber end or the coupler did not pass through the QWP; thus, they maintained the polarization state. The reflection light at the fiber end and the fiber coupler could be rejected through the PBS.

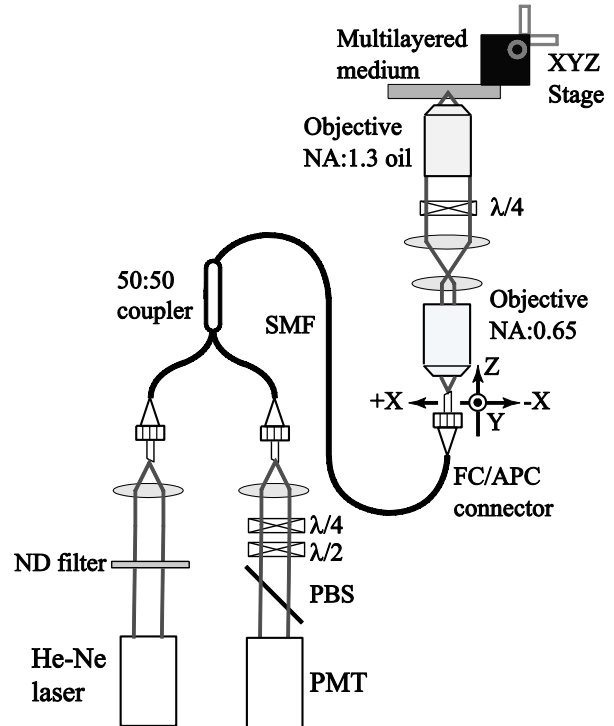


Fig. 7 Optical setup of fiber confocal microscope

VI. VERIFICATION OF AXIAL RESOLUTION OF FIBER CONFOCAL MICROSCOPE

We verified the axial resolution of the fiber confocal microscope using a multilayered sample. Figure 8 shows the structure of the multilayered sample. The multilayered sample was fabricated with high-refractive-index (HRI) layers and buffer layers. The top was the cover layer, and the bottom was a glass substrate. The refractive indexes of the HRI layers, the buffer layers, and the cover layer were 1.53, 1.466, and 1.518 at a wavelength of 633 nm, respectively. The thicknesses of the HRI layers, the buffer layers, and the cover layer were 1, 10, and 5 μm , respectively. The medium had five HRI

layers. The HRI layers were prepared with poly(methyl methacrylate) (PMMA). The buffer layers were prepared with butyl acrylate and acrylic acid, and the cover layer was prepared with poly(vinyl alcohol) (PVA).

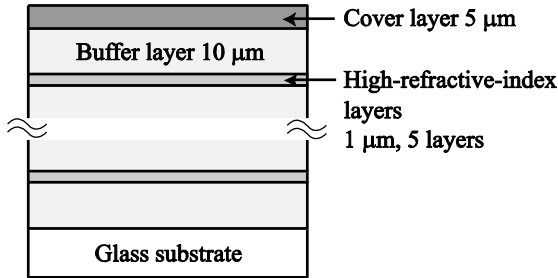


Fig. 8 Structure of multilayered sample for performance evaluation of fiber confocal microscope

Figure 9(a) shows the axial response of the multilayered sample. We could observe the reflection peaks of the HRI layers. The rightmost peak corresponded to the interface between the cover layer and the buffer layer. The five center peaks indicated the HRI and buffer layer interfaces, and the leftmost peak represented the reflection from the interface between the buffer layer and the glass substrate.

Figure 9(b) shows the magnified image of the first HRI layer peak shown in Fig. 9(a). The full width at half maximum (FWHM) of this peak was 900 nm. Therefore, we considered that the axial resolution of the fiber confocal microscope was 900 nm.

Figure 9(c) shows the axial response of the same sample before the introduction of the two noise reduction methods. The background noise level was higher and fluctuated as shown in Fig. 9(c). It is difficult to distinguish the interface between the cover layer and the buffer layer, from that between the buffer layer and the substrate. We succeeded in improving the signal-to-noise ratio (SNR) of the fiber confocal microscope to a level enabling the use of the microscope as the readout system of multilayered memories.

VII. VERIFICATION OF ALIGNMENT-FREE PERFORMANCE

We verified the alignment-free performance of the fiber confocal readout system. We used aligned

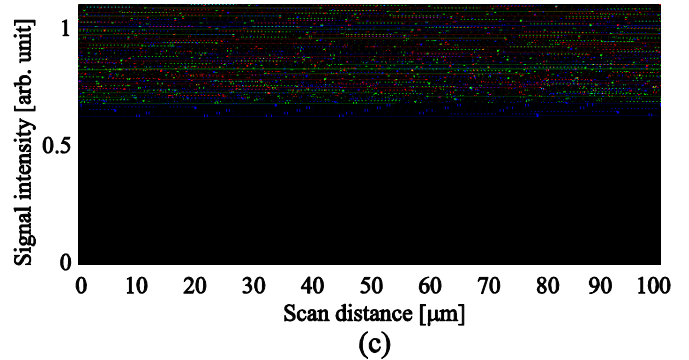


Fig. 9 Axial response of multilayered sample: (a) axial response with noise reduction methods, (b) magnified image of first peak shown in Fig. 9(a), and (c) axial response without noise reduction methods

latex spheres as reference samples. The fiber end was shifted from the optical axis in order to verify the alignment-free performance. The shift range of the fiber end was from plus 5 μm to minus 5 μm . The fiber end was shifted on the X-axis defined in Fig. 7. The latex spheres were aligned with the hexagonal close-packed structure on the glass substrate using the self-organization process. The diameter of the latex spheres was 10 μm .

Figure 10 shows the observation results of the latex spheres. Figure 10(a) shows the image of the minus 5 μm shift, Fig. 10(b) shows the latex spheres well aligned to the optical axis, and Fig. 10(c) shows the image of the plus 5 μm shift.

Images could be acquired in the case of misalignment. From these images, we confirmed that the fiber confocal microscope relaxes the required accuracy of the alignment of the fiber position. Comparing Figs. 10(b) and 10(c), the signal intensity in Fig. 10(c) was found to be approximately 32 % lower than that in Fig. 10(b). The degradation observed in Figs. 10(a) and 10(c) was caused by reducing the amount of light incident to the objective. The misalignment does not decrease the spatial resolution of the observed image if we use an aberration-free objective. In an actual case, the aberration and physical size of the objective determine the alignment-free capability range. The fiber confocal microscope also relaxes the required accuracy of the alignment in the axial direction; however, a severe spherical aberration is expected in this case.

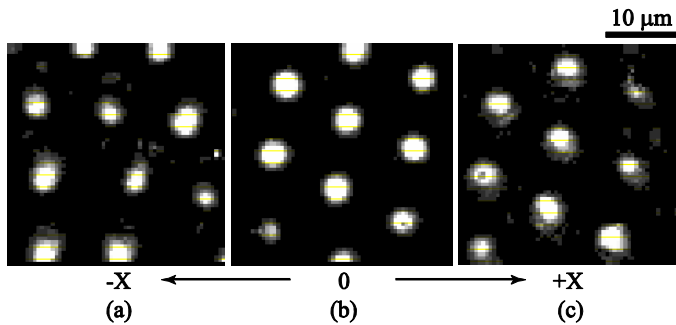


FIG. 10 OBSERVATION IMAGES OF 10 μm LATEX SPHERES: (A) -5 μm SHIFT OF FIBER END FROM THE OPTICAL AXIS, (B) LATEX SPHERES WELL ALIGNED TO THE OPTICAL AXIS, AND (C) +5 μm SHIFT

VIII. MULTILAYER RECORDING AND READOUT USING FIBER CONFOCAL MICROSCOPE

We recorded bit data into the multilayered recording medium and read them out using the fiber confocal microscope. A mode-locked Ti:sapphire laser was used to demonstrate the multilayer recording. Figure 11 shows the structure of the multilayered recording medium that we used. The multilayered medium consisted of ten recording layers and eleven buffer layers. The top was a PVA cover layer, and the bottom was a poly(ethylene terephthalate) (PET) substrate. The thickness of the recording layers, the buffer layers, and the cover layer were 1, 5, and 1 μm , respectively. The recording layers were prepared with PMMA. The photochromic DE was doped in PMMA. The composition of DE was *cis*-1,2-dicyano-1,2-

bis(2,4,5-trimethyl-3-thienyl)ethene. The concentration of DE as the recording material was 10% by weight. The multilayered recording medium was fabricated using a lamination process[13].

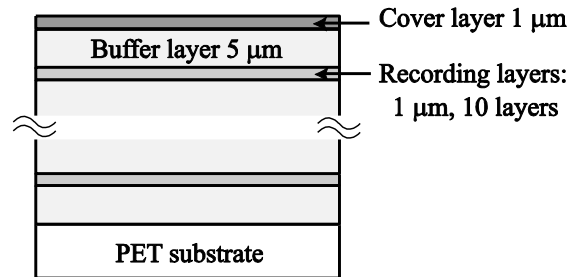


Fig. 11 Structure of multilayered recording medium

Figure 12 shows the multilayer recording and readout results obtained using the fiber confocal microscope. The bright and dark parts indicate the signal from the bit data and the reflection from the recording layer interfaces. We could achieve the eight-layer recording and readout. The alphabet patterns of each layer were recorded with the sequence of bit data. The bit interval was 2 μm . The average power and the exposure time were 61 mW and 8 ms, respectively. The low contrast shown in the first layer was caused by the lens aberration.

Figure 13(a) shows the axial response of the multilayered recording medium before recording. All recording layers could be detected using the fiber confocal microscope. The highest peak represented the reflection at the buffer layer and PET substrate interface. Figure 13(b) shows the axial cross section of the multilayered recording medium after recording. The bottom white line represents the interface of the buffer layer and the PET substrate, and the top line represents the interface of the cover layer and the buffer layer. The ten lines between the cover layer and the PET substrate interfaces indicate the recording layer interfaces. The recorded bits could be detected in the recording layers. Figure 14 shows the signal intensity distribution along the white line on the first layer. The dotted line indicates the reflection level from the recording layer interfaces. The signal level from the recording bits was higher than the reflection level from the recording layer interfaces. From the result shown in Fig. 14, we estimated that

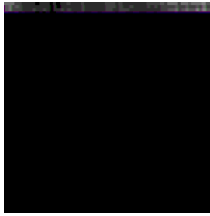


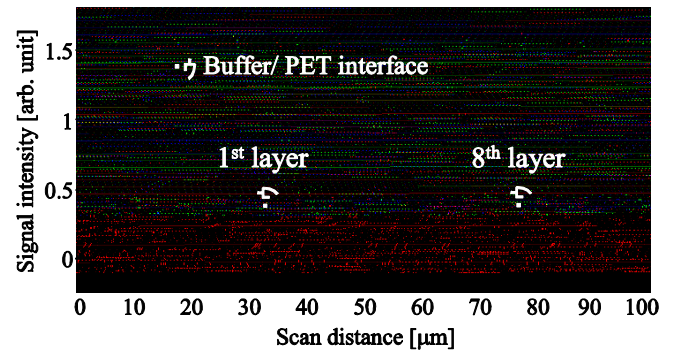
Fig. 12 Multilayer recording and readout results using fiber confocal microscope

the SNR was over 22 dB. This is enough SNR to distinguish each bit from background noise. We may say that the fiber confocal microscope has a promising potential as the readout system of multilayered optical memories.

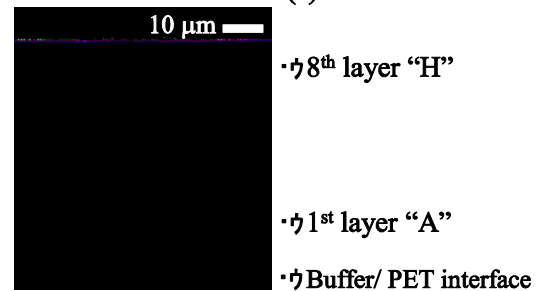
IX. CONCLUSIONS

We developed a compact and high-power mode-locked fiber laser for multilayered optical memories. The average power, repetition rate, and pulse width of the fiber laser that we developed were 109 mW, 57.5 MHz, and 2.1 ps, respectively. In order to increase the probability of the two photon process, we decreased the pulse width from 2.1 ps to 93 fs by pulse compression using a SMF. The average power at the SMF end was 90 mW and the peak power was 5.3 kW.

We also developed a fiber confocal microscope as a readout system of multilayered optical memories. The axial resolution of the fiber confocal microscope was 900 nm. We verified the



(a)



(b)

Fig. 13 (a) Axial response of multilayered recording medium before recording. (b) Axial cross section of multilayered recording medium after recording



Fig. 14 Signal intensity distribution at white line on first layer.

alignment-free performance of the fiber confocal microscope.

We demonstrated the reading of bit data from a multilayered recording medium by using the fiber confocal microscope. The fiber confocal microscope could read out the bit data without crosstalk. As a result of these, we may say that the fiber confocal microscope is very promising to be a feasible as compact readout system of multilayered optical memories.

ACKNOWLEDGMENT

We are very grateful to LINTEC Corporation for providing us with the multilayered sample for the axial resolution measurement and the multilayered

recording medium for the multilayer recording.

REFERENCES

- [1] L. Dhar, A. Hale, H. E. Katz, M. L. Schilling, M. G. Schnoes, and F. C. Schilling, "Recording Media that Exhibit High Dynamic Range for Digital Holographic Data Storage," *Opt. Lett.* **24** (1999) 487.
- [2] H. Horimai, X. Tan, and J. Li, "Collinear Holography," *Appl. Opt.* **44** (2005) 2575.
- [3] M. Shinoda, K. Saito, T. Ishimoto, T. Ito, A. Nakaoki, M. Yamamoto, O. Maeda, T. Hashizu, T. Asano, K. Aga, K. Takagi, and M. Tazoe, "High Density Near-Field Optical Disc System," *Jpn. J. Appl. Phys.* **45** (2006) 1321.
- [4] J. Tominaga, H. Fuji, A. Sato, T. Nakano, T. Fukaya, and N. Atoda, "The Near-Field Super-Resolution Properties of an Antimony Thin Film," *Jpn. J. Appl. Phys.* **37** (1998) L1323.
- [5] S. Kawata and Y. Kawata, "Three-Dimensional Optical Data Storage Using Photochromic Materials," *Chem. Rev.* **100** (2000) 1777.
- [6] T. Tanaka, K. Yamaguchi, and S. Yamamoto, "Rhodamine-B-doped and Au(III)-doped PMMA film for three-dimensional multi-layered optical memory," *Opt. Commun.* **212** (2002) 45.
- [7] M. Gu and D. Day, "Use of continuous-wave illumination for two-photon three-dimensional optical bit data storage in a photobleaching polymer," *Opt. Lett.* **24** (1999) 288.
- [8] T. Shiono, T. Itoh, and S. Nishino, "Two-Photon Absorption Recording in Photochromic Diarylethenes Using Laser Diode for Three-Dimensional Optical Memory," *Jpn. J. Appl. Phys.* **44** (2005) 3559.
- [9] F.-H. Wu, H.-P. Shieh, T. D. Milster, and D.-R. Huang, "Write-Once Volumetric Optical Disk Using Transparent Recording Material with an Optical Switching Layer," *Jpn. J. Appl. Phys.* **43** (2004) 4937.
- [10] M. Ogasawara, K. Takahashi, M. Nakano, M. Inoue, A. Kosuda, and T. Kikukawa, "16 Layers Write Once Disc with a Separated Guide Layer," presented at Int. Symp. Optical Memory 2010, Th-L-07.
- [11] T. Takuo, "Plasmon Enhanced Three-Dimensional Multi-Layer Optical Disk," presented at Int. Symp. Optical Memory 2010, Mo-D-02.
- [12] P. Zijlstra, J. W. M. Chon, and M. Gu, "Five-Dimensional Optical Recording Mediated by Surface Plasmons in Gold Nanorods," *Nature* **459** (2009) 410.
- [13] M. Miyamoto, M. Nakano, M. Nakabayashi, S. Miyata, and Y. Kawata, "Fabrication of Multilayered Photochromic Memory Using Pressure Sensitive Adhesives," *Appl. Opt.* **45** (2006) 8424.